

Voltage profile and four-terminal resistance of an interacting quantum wire

Liliana Arrachea

Departamento de Física de la Materia Condensada and BIFI, Universidad de Zaragoza, Pedro Cerbuna 12, 50009 Zaragoza, Spain and Departamento de Física, FCEyN, UBA, Pabellón 1 Ciudad Universitaria, 1428 Buenos Aires, Argentina

Carlos Naón and Mariano Salvay

Departamento de Física, Facultad de Ciencias Exactas, Universidad Nacional de La Plata and IFLP-CONICET, CC 67, 1900 La Plata, Argentina

(Received 22 November 2007; published 24 June 2008)

We investigate the behavior of the four-terminal resistance $R_{4\text{pt}}$ in a quantum wire described by a Luttinger liquid in two relevant situations: (i) in the presence of a single impurity within the wire and (ii) under the effect of asymmetries introduced by disordered voltage probes. In the first case, interactions leave a signature in a power-law behavior of $R_{4\text{pt}}$ as a function of the voltage V and the temperature T . In the second case interactions tend to mask the effect of the asymmetries. In both scenarios the occurrence of negative values of $R_{4\text{pt}}$ is explained in simple terms.

DOI: [10.1103/PhysRevB.77.233105](https://doi.org/10.1103/PhysRevB.77.233105)

PACS number(s): 73.63.Nm, 72.10.Bg, 73.23.-b, 73.63.Fg

The proposal of a fundamental relation between the two terminal conductance G and the universal quantum $G_0 = e^2/h$ is one of the milestones of electronic quantum transport in mesoscopic systems.^{1,2} For noninteracting electrons, such a relation explicitly reads $G = nG_0$, with n the number of electronic channels.² The same relation has been later theoretically and experimentally proved to be also valid in the case of wires of interacting electrons of finite length ideally attached to noninteracting leads.^{3,4}

Experiments in single-wall nanotubes (SWNTs), ropes of SWNTs, and also in multiple-wall nanotubes (MWNTs)⁵ have instead identified that the tunneling conductance to metallic contacts G_t follows a power-law behavior with the voltage V , $G_t \propto V^\alpha$ at low temperature T , and $G_t \propto T^\alpha$ for low V . The exponent α is a function of the forward electron-electron (e-e) interaction g . These features can be understood within the framework of a Luttinger liquid (LL) theory by means of theoretical treatments⁶ going beyond linear response in V and T .

Recently, a combined structure of MWNTs and SWNTs has been used to analyze the behavior of the four-point resistance $R_{4\text{pt}}$ of a SWNT.⁷ The total resistance of a mesoscopic system in a two terminal setup contains the component $1/G_0$ due to the coupling to the reservoirs. Instead, $R_{4\text{pt}}$ is expected to characterize the genuine resistance of the sample. For noninteracting electrons at low V and zero temperature, Büttiker has elaborated the concept of the multiterminal resistance within scattering-matrix theory (SMT),⁸ emphasizing the role of the symmetries. Although a naive expectation would be $R_{4\text{pt}} \geq 0$, this theory predicts also the possibility of $R_{4\text{pt}} < 0$ as a consequence of quantum interference effects. This remarkable feature has been experimentally observed.^{7,9}

While the consequences of elastic scattering due to impurities can be analyzed in terms of noninteracting electrons, the role of the e-e interaction in the behavior of $R_{4\text{pt}}$ remains an open question. The proper evaluation of this quantity implies dealing with a multiterminal setup as the one sketched in Fig. 1, which is difficult to implement within theoretical approaches such as those of Refs. 6, 10, and 11. Previous multiterminal treatments in LL rely on the effective reduc-

tion to a noninteracting model by recourse to a Hartree-Fock decoupling of the interaction term¹² or focus in linear response in V (Ref. 13). In this work we use Keldysh nonequilibrium Green's functions, which are a convenient framework to tackle multiterminal geometries by exactly treating the e-e interaction while going beyond linear response. We analyze two relevant ingredients giving rise to a nontrivial behavior of the local potential μ_j and $R_{4\text{pt}}$: (i) the presence of an impurity in the wire and (ii) a clean wire probed by disordered leads with asymmetric densities of states.

We consider the setup sketched in Fig. 1, which consists in a quantum wire described by a Tomonaga-Luttinger model under the influence of a voltage V . Two reservoirs are in contact with the wire at the points x_1, x_2 through very weak ("noninvasive") tunneling constants. Their chemical potentials μ_1 and μ_2 satisfy the condition of a vanishing current through the ensuing contacts. In this way, a continuous current I flows through the wire, and

$$\frac{R_{4\text{pt}}}{R_{2\text{pt}}} = \frac{\mu_1 - \mu_2}{V}. \quad (1)$$

In the case of an ideal and clean wire with identical noninvasive probes, a simple analysis of the symmetries of the setup leads to $R_{4\text{pt}} = 0$. The full system is described by the action $S = S_{\text{wire}} + S_{\text{imp}} + S_{\text{res}} + S_{\text{cont}}$, where S_{res} describes the two reservoirs that constitute the voltage probes and S_{wire} is expressed in terms of right (r) and left (l) movers (in our system of units $\hbar = v_F = e = 1$):

$$S_{\text{wire}} = \int dx dt \{ \psi_r^\dagger [i(\partial_t + \partial_x) - \mu_r] \psi_r + \psi_l^\dagger [i(\partial_t - \partial_x) - \mu_l] \psi_l - g [\psi_r^\dagger \psi_r + \psi_l^\dagger \psi_l]^2 \}, \quad (2)$$

where g is the Luttinger e-e interaction in the forward channel while $\mu_r = \mu + V/2$ and $\mu_l = \mu - V/2$. The effect of the impurity is contained in the backscattering interaction,

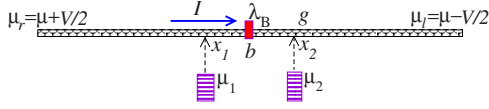


FIG. 1. (Color online) Sketch of the setup: A voltage V is imposed on a Luttinger liquid with a backscattering impurity of strength λ_B , through the chemical potentials for the left and right movers: $\mu_{r,l} = \mu \pm V/2$. Two voltage probes are connected at the positions x_1, x_2 . The corresponding chemical potentials $\mu_{1,2}$ are fixed by the condition of zero current through the contacts.

$$S_{\text{imp}} = \lambda_B \int dx dt \delta(x-b) [e^{-2ik_F x} \psi_r^\dagger \psi_l + \text{H.c.}]. \quad (3)$$

The term S_{cont} represents the tunneling between the reservoirs and the wire,

$$S_{\text{cont}} = \sum_{j=1,2,\alpha,\beta=l,r} \int dx dt w_j \delta(x-x_j) \times [e^{\mp i(k_F + k'_F)x} \psi_\alpha^\dagger \chi_{\beta,j} + \text{H.c.}], \quad (4)$$

where the fields $\chi_{\alpha,j}^\dagger$, with $\alpha, \beta = l, r$ and $j = 1, 2$ denote degrees of freedom of the reservoirs. The upper and lower sign corresponds to $\alpha = r$ and l , respectively. For simplicity, the dependence of the fields on x and t has been omitted in the above equations. At this point we carry out the gauge transformation $\psi_{l,r}^\dagger(x) \rightarrow e^{i\pm k_F x} \psi_\alpha^\dagger(x)$, where k_F is the Fermi vector of the electrons in the wire (a similar transformation involving k'_F is implemented with the fields $\chi_{\alpha,j}^\dagger$).

The tunneling currents through the contacts to the probes read

$$I_j = iw_j \sum_{\alpha,\beta=l,r} \langle \chi_{j,\alpha}^\dagger(x_j, t) \psi_\beta(x_j, t) - \text{H.c.} \rangle. \quad (5)$$

In what follows, we evaluate the currents I_j up to the first order of perturbation theory in the tunneling amplitudes. This procedure is appropriate in the limit of weak w_j , which is a reasonable assumption for measurements of $R_{4\text{pt}}$ with “non-invasive” probe leads.⁷ Within this lowest order of perturbation theory,

$$I_j = 2|w_j|^2 \sum_{\alpha,\beta=l,r} \int_{-\infty}^{+\infty} \frac{d\omega}{2\pi} [G_{\alpha,\beta}^>(x_j, x_j; \omega) G_j^<(\omega) - G_{\alpha,\beta}^<(x_j, x_j; \omega) G_j^>(\omega)], \quad (6)$$

where $G_{\alpha,\beta}^<(\omega)$ are the Fourier transforms with respect to $t - t'$ of the lesser and bigger Green's functions $G_{\alpha,\beta}^<(x, x'; t - t') = i \langle \psi_\beta^\dagger(x', t') \psi_\alpha(x, t) \rangle$ and $G_{\alpha,\beta}^>(x, x'; t - t') = -i \langle \psi_\alpha(x, t) \psi_\beta^\dagger(x', t') \rangle$, corresponding to the wire *uncoupled from the probes*, while $G_j^>(\omega) = \lambda_j^>(\omega) \rho_j(\omega)$ are the Green's functions of the uncoupled probe reservoirs, with $\lambda_j^<(\omega) = if(\omega - \mu_j)$, $\lambda_j^>(\omega) = -i[1 - f(\omega - \mu_j)]$, and $\rho_j(\omega)$ the ensuing density of states, which we assume to be identical for the two kinds of movers within these systems. The chemical potentials of the probes μ_j must be fixed to satisfy $I_j = 0$. Notice that within this order of perturbation theory the effect of the two probes is completely uncorrelated from one another since interference terms between the probes and re-

sistive effects involve second order processes in w_j (Ref. 14).

We now turn to analyze the first ingredient of interest, namely, the effect of an impurity in the wire. In terms of our model, this corresponds to consider a finite λ_B . We also consider a simple model for the probes, with a constant density of states $\rho_j(\omega) = \rho_0$. While the Green's functions of the uncoupled homogeneous interacting wire are known,¹⁵ the evaluation of the corresponding functions in the presence of a backscattering center is a nontrivial task. Below, we indicate the lines we have followed in order to evaluate them up to the first order of perturbation theory in λ_B . The expressions for the lesser and bigger Green's functions cast

$$G_{\alpha\beta}^>(\omega) = \delta_{\alpha\beta} \lambda_\alpha^>(\omega) \rho_{0,\alpha}(x - x', \omega) + \delta_{\bar{\alpha}\beta} \lambda_B \{ \lambda_\alpha^>(\omega) \rho_{0,\alpha}(x - b, \omega) \times [G_{0,\beta}^R(x' - b, \omega)]^* + \lambda_\beta^>(\omega) \times G_{0,\alpha}^R(x - b, \omega) \rho_{0,\beta}(b - x', \omega) \}, \quad (7)$$

with $\bar{l} = r, \bar{r} = l$, $\lambda_\alpha^<(\omega) = if(\omega - \mu_\alpha)$, and $\lambda_\alpha^>(\omega) = -i[1 - f(\omega - \mu_\alpha)]$. The spectral density,

$$\rho_{0,\alpha}(x, \omega + \mu_\alpha) = C_\psi \exp \left[\mp i \left(\frac{\omega}{v} - k_F \right) x \right] \times |\omega|^{2\gamma} \phi \left(\gamma, 2\gamma + 1, \pm 2ix \frac{\omega}{v} \right), \quad (8)$$

corresponds to the clean LL uncoupled from the probes, where $v = \sqrt{1 + 2g/\pi}$ is the renormalized Fermi velocity and $\phi(a, b; c)$ is Kummer's hypergeometric function. The exponent $\gamma = (K + K^{-1} - 2)/4$ ($K = 1/v$) is determined by g . The retarded Green's functions are defined from the Kramers-Kronig relation, being $\rho_{0,\alpha}(x, \omega) = -2 \text{Im}[G_{0,\alpha}^R(x, \omega)]$. In order to perform numerical computations we introduce an energy cutoff Λ by replacing $\rho_{0,\alpha}(x, \omega + \mu_\alpha) \rightarrow \Theta(|\omega| - \Lambda) \rho_{0,\alpha}(x, \omega + \mu_\alpha)$. Therefore, the constant C_ψ is a function of Λ , which is determined by the sum rule $\int_{-\infty}^{+\infty} d\omega \rho_{\alpha,0}(0, \omega) = 2\pi$.

Substituting the above expressions in (6) gives the following result for the currents through the contacts:

$$I_j(x_j) = 2|w_j|^2 \sum_{\alpha=l,r} \int_{-\infty}^{+\infty} \frac{d\omega}{2\pi} [f(\omega - \mu_j) - f(\omega - \mu_\alpha)] \times \rho_j(\omega) \rho_\alpha^{\text{eff}}(x_j, \omega), \quad (9)$$

with

$$\rho_\alpha^{\text{eff}}(x_j, \omega) = \rho_{0,\alpha}(0, \omega) + 2\lambda_B \text{Re} \{ \rho_{0,\alpha}(x_j - b, \omega) \times [G_{0,\bar{\alpha}}^R(x_j - b, \omega)]^* \} \quad (10)$$

the effective density of states of the α movers (or the α injectivity¹⁶) at the position x_j of the wire, which contains the contribution of the local density of states of the homogeneous wire, $\rho_{0,\alpha}(0, \omega)$ plus a correction due to the backscattering by the impurity. It is important to note that $I_j(x_j) \propto \lambda_B$, while the current through the wire is $I \propto \lambda_B^2$ (see also Refs. 10 and 11). For $T=0$ and low V , the condition $I_j=0$ leads to

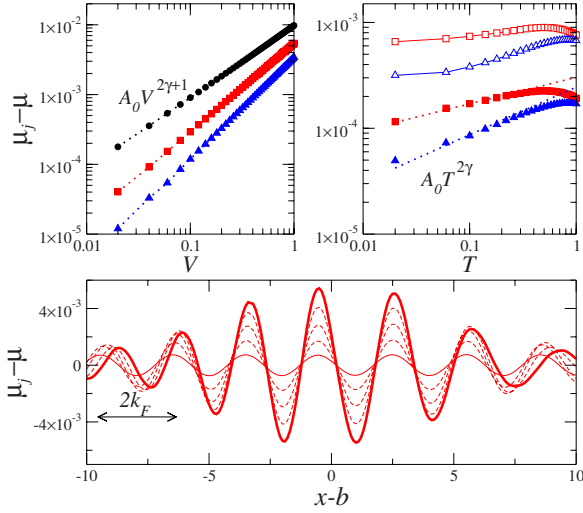


FIG. 2. (Color online) Behavior of the local potential μ_j for a wire with $\lambda_B=0.1$ as a function of the bias V for $T=0$ and $x_j=-0.2$ (upper left panel) and as a function of T for $V=0.2$ and $x_j=-0.2$ (right panel). Circles, squares, and triangles correspond to $K=1, 0.5,$ and $0.4,$ respectively. Solid and open symbols correspond to $V=0.05$ and $0.2,$ respectively (right panel). The fits with power laws are shown in dotted lines. Lower panel: μ_j as a function of $x-b$ for $V=0.2, \dots, 1$ and $K=0.5.$

$$\mu_j = \mu + \frac{V \rho_l^{\text{eff}}(x_j, \mu) - \rho_r^{\text{eff}}(x_j, \mu)}{2 \rho_l^{\text{eff}}(x_j, \mu) + \rho_r^{\text{eff}}(x_j, \mu)}, \quad (11)$$

where we have made use of the fact that $\rho_j(\omega)$ is constant and that $\rho_\alpha^{\text{eff}}(x_j, \omega) \sim \rho_\alpha^{\text{eff}}(x_j, \mu)$ within a small window $|\omega - \mu| \leq V/2.$ Equation (11) reduces to Eq. (37) of Ref. 16 for noninteracting electrons. It explicitly shows that the local potential monitors the difference between the left and right injectivities at point $x_j,$ relative to the total density of states at the given point. It is natural to expect that such an observable should provide valuable information on the Friedel oscillations introduced by the impurity,^{10,11,16,17} as well as on the strength of the e-e interactions. In fact, a low-energy expansion of the spectral densities casts

$$\begin{aligned} \mu_j &\sim \mu + C_1 \lambda_B \sin(2k_F x) V^{2\gamma+1}, \quad T=0, \\ \mu_j &\sim \mu + C_2 \lambda_B V \sin(2k_F x) T^{2\gamma}, \quad V \ll T, \end{aligned} \quad (12)$$

with C_1 and C_2 functions of $\gamma.$

The results of the full numerical calculation of μ_j from the condition of $I_j(x_j)=0$ for arbitrary voltage differences and temperature, with the exact effective density $\rho_\alpha^{\text{eff}}(x_j, \omega)$ [also evaluated numerically from Eq. (10)], are shown in Fig. 2. At $T=0,$ μ_j as a function of the distance to the impurity, shown in the lower panel, oscillates with the period $2k_F$ of the Friedel oscillations, with a voltage-dependent amplitude that follows the power law [Eq. (12)] (see upper left panel). For large distances to the impurity and high $V,$ beyond the scope of the approximations leading to Eq. (12), the pattern shows additional structure and the amplitude of the oscillations decreases with the distance to the impurity. The evolution of μ_j as the temperature increases, corresponding to two values of

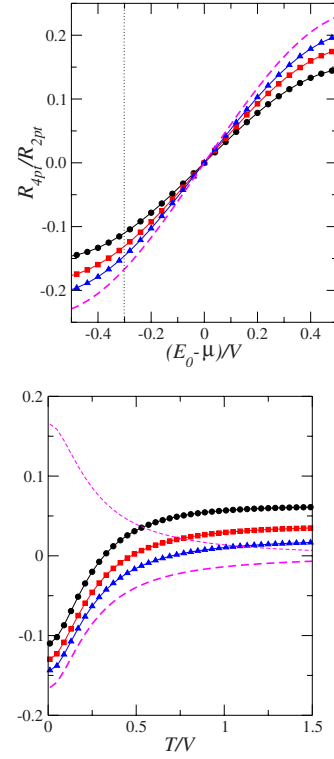


FIG. 3. (Color online) Four point resistance $R_{4\text{pt}}/R_{2\text{pt}}$ of a LL with interaction parameter K for a bias $\mu_r - \mu_l = V.$ The probe $j=1$ has a Lorentzian density of states (a resonance) with width $\Delta = 0.4V$ centered at $E_0.$ The probe $j=2$ has a constant density of states [which implies $\mu_2 = \mu = (\mu_l + \mu_r)/2.$] The top panel corresponds to temperature $T=0$ and shows the changes in $R_{4\text{pt}}$ at the center of the resonance is moved around $\mu.$ Circles, squares, and triangles correspond to $K=0.4, 0.5,$ and 0.6 while dashed lines correspond to the noninteracting case ($K=1.$) The bottom panel shows the evolution with the temperature for the value of $(E_0 - \mu)/V = -0.3$ indicated with dotted lines in the top panel. The thin dashed line corresponds to $K=1$ and $(E_0 - \mu)/V = 0.3.$

the voltage, is illustrated in the upper right panel of Fig. 2, where the dependence [Eq. (12)] is also verified within the low T and low V regime, with $V \ll T.$ From these features we can infer the behavior of $R_{4\text{pt}}/R_{2\text{pt}}$ along the sample by simply substituting Eq. (11) in Eq. (1). In particular, we conclude that as a function of $x,$ $R_{4\text{pt}}/R_{2\text{pt}}$ should follow the pattern of Friedel oscillations, being positive or negative, depending on the points at which the probes are connected. As a function of V it should be a power law with exponent $2\gamma.$ As a function of $T,$ it should present rapid changes within the range $T < V$ and a crossover to a power law with exponent 2γ at higher temperatures.

We now consider the second situation of interest: the wire without impurities ($\lambda_B=0$) but disordered probe leads. Thus, the expressions for the Green's function of the wire reduce to the ones for the homogeneous LL while the expression for the tunneling current of Eq. (6) reduces to Eq. (9) with $\rho_\alpha^{\text{eff}}(x_j, \omega) \equiv \rho_{\alpha,0}(0, \omega).$ While perfect metallic systems are expected to have approximately flat densities of states, impurities introduce effective barriers, generating peaks in the densities of states $\rho_j(\omega).$

Let us first analyze $T=0$ and probes with asymmetric densities of states, such that $\rho_j(\omega) \sim \rho_j^-(\mu)$, $\mu - V/2 \leq \omega \leq \mu$ and $\rho_j(\omega) \sim \rho_j^+(\mu)$, $\mu \leq \omega \leq \mu + V/2$. Then, the condition of a vanishing current [Eq. (6)] leads to

$$\mu_j = \mu + \frac{V}{2} \left[\frac{\rho_j^+(\mu)^\nu - \rho_j^-(\mu)^\nu}{\rho_j^-(\mu)^\nu + \rho_j^+(\mu)^\nu} \right], \quad (13)$$

with $\nu = 1/(2\gamma + 1)$. For probes with symmetric densities of states, we get $\mu_j = \mu$ and $R_{4\text{pt}} = 0$. Instead, for an asymmetric density of states, the potential drop between the highest potential r and the probe j is lower (higher) than the one between j and l for $\rho_j^-(\mu) > \rho_j^+(\mu)$ [$\rho_j^-(\mu) < \rho_j^+(\mu)$], respectively, which reflects the fact that the larger the spectral weight of the probe, the larger the ability of that element to introduce resistive effects. For finite temperature and very low voltage such that $T \gg V$, it can be verified that $\mu_j = \mu$, $j = 1, 2$, and $R_{4\text{pt}} = 0$.

Therefore, asymmetric densities of states of at least one of the probes together with the condition $\rho_1(\omega) \neq \rho_2(\omega)$ would lead to a nonvanishing $R_{4\text{pt}}$ when $T < V$. An example is analyzed in Fig. 3. We consider a Breit-Wigner model for one of the probes, assuming a single resonance within the window of width V centered around μ : $\rho_1(\omega) = A_1/[(\omega - E_0)^2 + \Delta]$, and a constant density of states $\rho_2 = A_2$ for the other probe, where A_1 and A_2 are normalization constants and $\mu - V/2 \leq E_0 \leq \mu + V/2$. Under these conditions $\mu_2 = \mu$, while μ_1 is determined to satisfy $I_1 = 0$. Results for the corresponding relative resistance $R_{4\text{pt}}/R_{2\text{pt}} = (\mu_1 - \mu_2)/V$ are shown in Fig. 3. The left panel corresponds to temperature $T = 0$. When the center of the resonance E_0 coincides with the mean chemical potential μ , the spectral weight spreads out symmetrically around this point. Thus, $\rho_1^+(\mu) = \rho_1^-(\mu)$ and $\mu_1 = \mu$, then $R_{4\text{pt}} = 0$. As the center of the resonance moves to lower energies, so does μ_1 and $R_{4\text{pt}}$ becomes negative. Conversely, for $E_0 > \mu$, it is obtained that $R_{4\text{pt}} > 0$. Remarkably, interactions tend to mask the structure observed in the noninteracting case (with $K = 1$).

The behavior of $R_{4\text{pt}}$ as a function of the temperature is shown in the right panel for the case $(E_0 - \mu)/V = -0.3$. Notice that the cases with $(E_0 - \mu)/V > 0$ can be obtained from the ones with $(E_0 - \mu)/V < 0$ by simply transforming $R_{4\text{pt}} \rightarrow -R_{4\text{pt}}$ in the figure. In all the cases, there is a range of temperature $T < V$, where $R_{4\text{pt}}$ experiments significant changes.

To conclude, let us comment on the theoretical and experimental impact of our results. When an impurity is in the wire, it induces Friedel oscillations that manifest themselves in the local voltage and $R_{4\text{pt}}$. The interactions leave a clear signature in the power-law behavior $R_{4\text{pt}}/R_{2\text{pt}} \propto V^{2\gamma}$ and $R_{4\text{pt}}/R_{2\text{pt}} \propto T^{2\gamma}$. Interestingly, the exponent is different from the one predicted in Ref. 11 for the two terminal conductance of a LL with an impurity. This result has a significant conceptual weight since it constitutes a concrete example of the fact that different fundamental processes contribute to each of these quantities ($R_{4\text{pt}}/R_{2\text{pt}} \propto \lambda_B$ while $G \propto \lambda_B^2$). Therefore, a genuine multiterminal setup is essential to evaluate $R_{4\text{pt}}$. For impurities in the probes and an asymmetric configuration, $R_{4\text{pt}}$ is determined by the way in which the density of states of the probe is distributed within an energy window of width V centered in μ while the e-e interactions play a milder role. In both cases, the behavior of $R_{4\text{pt}}$ as a function of temperature at a sizable V is highly nonuniversal and exhibits significant changes in the range $T < V$. These results should help to provide a theoretical framework to further analyze experimental data in SWNT, such as those of Ref. 7 as well as to guide additional experiments along that line in the future.

We thank A. Bachtold, M. Büttiker, and C. Chamon for useful discussions. We acknowledge support from CONICET, Argentina, Grants No. FIS2006-08533-C03-02 and No. PIP-6157; UNLP, Argentina, Grant No. PIA-11X386; and the ‘‘RyC’’ program from MCEyC, grant DGA for Groups of Excellence, and AUIP of Spain.

¹R. Landauer, Philos. Mag. **21**, 863 (1970).

²M. Büttiker, Y. Imry, R. Landauer, and S. Pinhas, Phys. Rev. B **31**, 6207 (1985).

³W. Apel and T. M. Rice, Phys. Rev. B **26**, 7063 (1982); C. L. Kane and M. P. A. Fisher, *ibid.* **46**, 15233 (1992); D. L. Maslov and M. Stone, *ibid.* **52**, R5539 (1995); V. V. Ponomarenko, *ibid.* **52**, R8666 (1995); I. Safi and H. J. Schulz, *ibid.* **52**, R17040 (1995).

⁴S. Tarucha, T. Honda, and T. Saku, Solid State Commun. **94**, 413 (1995); N. Agrait, A. Levy Yeyati, and J. M. van Ruitenbeek, Phys. Rep. **81**, 377 (2003), and references therein.

⁵M. Bockrath, D. H. Cobden, J. Lu, A. G. Rinzler, R. E. Smalley, L. Balents, and P. L. McEuen, Nature (London) **397**, 598 (1999); M. Monteverde and M. Nuñez-Regueiro, Phys. Rev. Lett. **94**, 235501 (2005).

⁶R. Egger and A. O. Gogolin, Phys. Rev. Lett. **79**, 5082 (1997).

⁷B. Gao, Y. F. Chen, M. S. Fuhrer, D. C. Glattli, and A. Bachtold, Phys. Rev. Lett. **95**, 196802 (2005).

⁸M. Büttiker, Phys. Rev. Lett. **57**, 1761 (1986); IBM J. Res. Dev. **32**, 317 (1988).

⁹R. de Picciotto, H. L. Stormer, L. N. Pfeiffer, K. W. Baldwin, and K. W. West, Nature (London) **411**, 51 (2001).

¹⁰R. Egger and H. Grabert, Phys. Rev. Lett. **77**, 538 (1996); Phys. Rev. B **58**, 10761 (1998).

¹¹F. Dolcini, B. Trauzettel, I. Safi, and H. Grabert, Phys. Rev. B **71**, 165309 (2005).

¹²S. Lal, S. Rao, and D. Sen, Phys. Rev. B **66**, 165327 (2002); S. Das, S. Rao, and D. Sen, *ibid.* **70**, 085318 (2004).

¹³C. Chamon, M. Oshikawa, and I. Affleck, Phys. Rev. Lett. **91**, 206403 (2003); C.-Y. Hou and C. Chamon, Phys. Rev. B **77**, 155422 (2008).

¹⁴V. A. Gopar, M. Martinez, and P. A. Mello, Phys. Rev. B **50**, 2502 (1994); J. L. D’Amato and H. M. Pastawski, *ibid.* **41**, 7411 (1990).

¹⁵V. Meden and K. Schönhammer, Phys. Rev. B **46**, 15753 (1992); J. Voit, *ibid.* **47**, 6740 (1993).

¹⁶T. Gramspacher and M. Büttiker, Phys. Rev. B **56**, 13026 (1997).

¹⁷M. Büttiker, Phys. Rev. B **40**, 3409 (1989).